

Synthesis and Evaluation of Biological and Antitumor Activities of Tetrahydrobenzothieno[2,3-d]Pyrimidine Derivatives as Novel Inhibitors of FGFR1

Xuebao Wang^{1,†}, Di Chen^{1,†}, Shufang Yu¹,
Zaikui Zhang¹, Yu Wang¹, Xiaolu Qi², Weitao Fu¹,
Zixin Xie¹ and Faqing Ye^{1,*}

¹School of Pharmaceutical Sciences, Wenzhou Medical University, Wenzhou 325035, China

²Yichang Humanwell Pharmaceutical Co., Ltd, Yichang 443005, China

*Corresponding author: Faqing Ye, yfq664340@163.com

[†]These authors contribute equally to this work.

A series of tetrahydrobenzothieno[2,3-d]pyrimidine derivatives were designed, synthesized, and evaluated as inhibitors of FGFR1. These analogs were synthesized via Gewald's reaction under mild conditions. The structures of the synthesized compounds were characterized by spectroscopic data (IR, ¹H NMR and MS). Their antitumor activities were evaluated against H460, A549 and U251 cell lines *in vitro*. Results revealed that the tested compounds showed moderate antitumor activities. Structure–activity relationship analyses indicated that compounds with an aromatic ring substituted in the C-2 position or with larger molecules such as **3g**, **4c**, and **7** were more effective than others. The compound, **3g** (78.8% FGFR1 inhibition at 10 μ M), was identified to have the most potent antitumor activities, with *IC*₅₀ values of 7.7, 18.9, and 13.3 μ M against the H460, A549, and U251 cell lines, respectively. Together, the results suggested that tetrahydrobenzothieno[2,3-d]pyrimidine derivatives may serve as a potential agent for the treatment of FGFR1-mediated cancers.

Key words: antitumor, FGFR1, Gewald's reaction, synthesis, thieno[2,3-d]pyrimidine

Received 21 May 2015, revised 27 August 2015 and accepted for publication 2 October 2015

Highlights

- Designed and synthesized a series of tetrahydrobenzothieno[2,3-d]pyrimidine derivatives.
- Compound **3g** was identified to have the most potent antitumor activities, with *IC*₅₀ values of 7.7, 18.9 and

13.3 μ M against H460, A549 and U251 cell lines, respectively, along with 78.8% FGFR1 inhibition at 10 μ M.

- Compound **3g** could be a lead compound for design of FGFR1 inhibitors.

Protein tyrosine kinases play an important role in the signaling pathways that control cell proliferation and differentiation. Among these, receptor tyrosine kinases (RTKs) have been shown to be important mediators of signal transduction in cells (1–7). RTKs are important therapeutic targets for cancer drug discovery and development.

Fibroblast growth factor receptors (FGFRs) constitute a major class of RTKs serving as high-affinity receptors. FGFR1 is the founding member of the FGFR family and is known to be overexpressed in prostate carcinoma cells, breast carcinoma cells, lung cancer cells, and also other cancer cells (8,9). Given the pivotal role of FGFR1 in human cancers, the pathway of cancer development through FGFR1 overexpression and activation was targeted and analyzed. In the presence of tyrosine kinase inhibitors, cell proliferation would be blocked by preventing ATP from binding to the RTKs (10,11). Previous studies had shown the importance of ATP-binding by FGFR1 for its enzymatic activity (3,12). However, the *in vivo* efficacy of these FGFR inhibitors was limited by their rapid blood clearance (13). Furthermore, some FGFR1 inhibitors failed to enter into the market because of their high toxicity, such as PD173074, SU5402, and Brivanib (14–16). Based on the above considerations, a new class of tyrosine kinase inhibitors was designed in this study to mimic ATP and block the constitutive activation of FGFR1, thereby blocking the FGFR1-dependent cancer signaling pathway.

In the present, indoles and quinolones are the most studied small molecule inhibitors toward FGFR1, while thienopyrimidines occupy a special position because of their broad spectrum of biological activities. The thieno [2,3-d]pyrimidine ring was considered to show potential antitumor activity (17–19). Compound **16** which also has such a structure (Figure 1) was found to show inhibitory activity toward FGFR1 kinase with an *IC*₅₀ value of 50 μ M (20). Tetrahydrobenzothienopyrimidine has a good representation of five- and six-membered heterocycles including

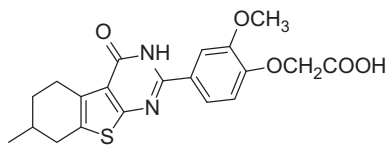


Figure 1: The Chemical structure of compound **16**.

six with fused polycyclic ring systems, the polycyclic cores overlap the position of adenine of ATP when bound, and meanwhile, the complexes feature hydrogen bonds in the hinge region. In other words, the substitution of the C-2 position can occupy hydrophobic pocket II so that the ATP cannot bind with receptors. Given these findings, compound **16** was chosen as a lead compound, and derivatives were synthesized to see if a simple analog in a low μM range could be obtained.

The lactam structure of tetrahydrobenzothienopyrimidine was considered to be a key group because of the ability to form hydrogen bonds. Taking this into account, we considered whether amino was better than carbonyl group, as amino group could act both hydrogen bond donor and hydrogen bond acceptor. Here, in this manuscript, compounds with amino group in tetrahydrobenzothienopyrimidine were named series 1, while compounds with carbonyl were named series 2. Series 2 were designed to compare with series 1.

Methods and Materials

General

All organic chemicals were available commercially and used without further purification. The reagents and anhydrous solvents were purchased from Aladdin and Sinopharm Chemical Reagent Co., Ltd. All melting points (m.p.) were uncorrected and measured using an XRC-1 micromelting point apparatus. The thin layer chromatography (TLC, R_f values) was performed on F₂₅₄ or silica gel plates F₂₅₄ (0.2 mm thick) and visualization of the spots was effected by exposure to UV light. The IR spectra were recorded on a Bruker Nicolet 670FT-IR spectrophotometer using KBr pellets. ¹H-NMR spectra were determined on a Bruker Avance III Spectrometer (600 MHz). Samples were dissolved in DMSO-*d*₆ or CDCl₃ while TMS was used as internal standard. Chemical shifts were recorded in (ppm) values relative to TMS and *J* values are expressed in Hertz. Splitting patterns were designated as follows: s, singlet; d, doublet; t, triplet. Mass spectra were recorded using an Agilent-1200 LC-MS Spectrometer. Elemental analyses were performed on a Thermo Scientific Elemental Analyzer Flash EA 1112 and were found within $\pm 0.4\%$ of the theoretical values.

For convenience in the manuscript, TBTP was used to represent 5,6,7,8-tetrahydrobenzo-[4,5]thieno[2,3-d]pyrimidine.

Chemistry

Synthesis of 2-amino-4,5,6,7-tetrahydrobenzo[2,3-b]thiophene-3-carbonitrile (**1**)

2-Amino-4,5,6,7-tetrahydrobenzo[2,3-b]thiophene-3-carbonitrile (**1**) was prepared by means of Gewald's reaction as reported in the literature (20–22). Formation of 2-amino-4,5,6,7-tetrahydrobenzo[2,3-b]thiophene-3-carbonitrile (**1**) was characterized by the presence of a band at 2210 cm^{-1} due to a cyano group and N–H stretching bands at 3325 and 3209 cm^{-1} in their IR spectra.

Synthesis of 4-amino-2-chloromethyl-5,6,7,8-tetrahydrobenzo[4,5]thieno[2,3-d]pyrimidine (**2**)

A mixture of 2-amino-4,5,6,7-tetrahydro-1-benzothienophene-3-carbonitrile **1** (1 g, 52 mmole) and chloroacetonitrile (1 mL) in dioxane (15 mL) was heated at 80 °C for 10 min; then, 20 mL of concentrated hydrochloric acid was added and reacted for 6 h. On completion of reaction (TLC), the mixture was cooled and poured onto cold water. The mixture then basified with ammonium hydroxide. The solid obtained was filtered, washed by methanol, dried, and crystallized from DMF to give **2** as a brown crystalline solid (62.4%).

General procedure for synthesis of compounds 3a–g

A mixture of compound **2** (0.2 mmol) and the corresponding amine (0.8 mmol) in dioxane (10 mL) was refluxed for 18 h. On completion of reaction (TLC), the solution was concentrated under reduced pressure and the residue was purified by column chromatography on silica gel (Ethyl acetate/petroleum ether).

4-Amino-2-[(diethylamino)methyl]-5,6,7,8-tetrahydrobenzo[4,5]thieno[2,3-d]pyrimidine (**3a**)

Pale yellow solid, Yield: 50.6%; mp 178–181 °C; IR (cm^{-1}): 3519 (NH₂). ¹H-NMR (CDCl₃): δ 1.10 (m, 6H, (CH₂CH₃)₂), 1.87–1.92 (m, 4H, TBTP-H), 2.69–2.72 (m, 4H, N(CH₂CH₃)₂), 2.78–2.81 (m, 2H, TBTP-H), 2.89–2.92 (m, 2H, TBTP-H), 3.75 (s, 2H, –CH₂–N–), 5.44 (s, 2H, –NH₂). EI-MS: 290.9[M + H]⁺. Calcd. For C₁₅H₂₂N₄S: C, 62.03; H, 7.64; N, 19.29; S, 11.04%. Found: C, 62.09; H, 7.55; N, 19.22; S, 11.14%.

4-Amino-2-[(piperidin-1-yl)methyl]-5,6,7,8-tetrahydrobenzo[4,5]thieno[2,3-d]pyrimidine (**3b**)

Pale yellow solid, Yield: 53.1%; mp 175–177 °C; IR (cm^{-1}): 3380 (NH₂). ¹H-NMR (CDCl₃): δ 1.50–1.55 (m, 6H, piperidin-H), 1.71–1.95 (m, 4H, TBTP-H), 2.73–2.84 (m, 2H, TBTP-H), 2.86–2.93 (m, 2H, TBTP-H), 3.62–3.69 (m, 4H, N(CH₂)₂), 3.81 (s, 2H, –CH₂–piperidin), 5.45 (s, 2H, –NH₂). EI-MS: 303.2[M + H]⁺. Calcd. For C₁₆H₂₂N₄S: C,

63.54; H, 7.33; N, 18.53; S, 10.60%. Found: C, 63.50; H, 7.37; N, 18.45; S, 10.68%.

4-Amino-2-[(morpholino-1-yl)methyl]-5,6,7,8-tetrahydrobenzo[4,5]thieno[2,3-d]pyrimidine (3c)

Pale yellow solid, Yield: 51.7%; mp 195–198 °C; IR (cm⁻¹): 3,499 (NH₂). ¹H-NMR (CDCl₃): δ 1.75–1.95 (m, 4H, TBTP-H), 2.60 (m, 4H, morpholine-H), 2.73–2.84 (m, 2H, TBTP-H), 2.86–2.93 (m, 2H, TBTP-H), 3.65–3.72 (m, 4H, morpholine-H), 3.81 (s, 2H, –CH₂–morpholine), 5.46 (s, 2H, –NH₂). EI-MS: 305.1[M + H]⁺. Calcd. For C₁₅H₂₀N₄O₂S: C, 59.18; H, 6.62; N, 18.41; O, 5.26; S, 10.53%. Found: C, 59.24; H, 6.64; N, 18.36; S, 10.52%.

4-Amino-2-[(4-methylpiperazin-1-yl)methyl]-5,6,7,8-tetrahydrobenzo[4,5]thieno[2,3-d]pyrimidine (3d)

Pale yellow solid, Yield: 61.3%; mp 210–212 °C; IR (cm⁻¹): 3440 (NH₂). ¹H-NMR (CDCl₃): δ 1.75–1.95 (m, 4H, TBTP-H), 2.28 (s, 3H, N–CH₃), 2.45 (m, 4H, piperazin-H), 2.62 (m, 4H, piperazin-H), 2.73–2.84 (m, 2H, TBTP-H), 2.86–2.93 (m, 2H, TBTP-H), 3.81 (s, 2H, –CH₂–piperazin), 5.60 (s, 2H, –NH₂). EI-MS: 318.0[M + H]⁺. Calcd. For C₁₆H₂₃N₅S: C, 60.54; H, 7.30; N, 22.06; S, 10.10%. Found: C, 60.50; H, 7.34; N, 22.06; S, 10.10%.

4-Amino-2-[(cyclohexylamino)methyl]-5,6,7,8-tetrahydrobenzo[4,5]thieno[2,3-d]pyrimidine (3e)

Pale yellow solid, Yield: 46.9%; mp 221–223 °C; IR (cm⁻¹): 3443 (NH₂). ¹H-NMR (CDCl₃): δ 1.12–1.20 (m, 4H, cyclohexyl-H), 1.23–1.35 (m, 4H, cyclohexyl-H), 1.56–1.61 (m, 2H, cyclohexyl-H), 1.73–1.89 (m, 4H, TBTP-H), 2.02 (s, 1H, –NH–), 2.25–2.27 (m, 1H, cyclohexyl-H), 2.73–2.84 (m, 2H, TBTP-H), 2.86–2.93 (m, 2H, TBTP-H), 3.89 (s, 2H, –CH₂–NH–), 5.38 (s, 2H, –NH₂). EI-MS: 317.2[M + H]⁺. Calcd. For C₁₇H₂₄N₄S: C, 64.52; H, 7.64; N, 17.70; S, 10.13%. Found: C, 64.55; H, 7.60; N, 17.73; S, 10.12%.

4-Amino-2-[N-(3-carboxyphenyl)aminomethyl]-5,6,7,8-tetrahydrobenzo[4,5]thieno[2,3-d]pyrimidine (3f)

White solid, Yield: 35.7%; mp 185–187 °C; IR (cm⁻¹): 3457 (NH₂). ¹H-NMR (DMSO-*d*₆): δ 1.73–1.89 (m, 4H, TBTP-H), 2.73–2.84 (m, 2H, TBTP-H), 2.86–2.93 (m, 2H, TBTP-H), 3.90 (s, 2H, –CH₂–NH–), 5.44 (s, 2H, –NH₂), 6.89 (s, 1H, –NH–), 6.83–7.20 (m, 4H, Ph-H), 11.45 (s, 1H, –COOH). EI-MS: 354.8[M + H]⁺. Calcd. For C₁₈H₁₈N₄O₂S: C, 61.00; H, 5.12; N, 15.81; S, 9.05%. Found: C, 61.06; H, 5.04; N, 15.83; S, 9.01%.

N'-[(4-amino-5,6,7,8-tetrahydrobenzo[4,5]thieno[2,3-d]pyrimidin-2-yl)methyl]isonicotinohydrazide (3g)

Yellow solid, Yield: 43.5%; mp >250 °C; IR (cm⁻¹): 3436 (NH₂), 1639 (C=O). ¹H-NMR (DMSO-*d*₆): δ 1.73–1.89 (m, 4H, TBTP-H), 2.73–2.84 (m, 2H, TBTP-H), 2.86–2.93 (m, 2H, TBTP-H), 3.91 (s, 2H, –CH₂–NH–), 5.74 (s, 1H, NHNHCO), 6.83 (s, 2H, –NH₂), 7.72 (d, 2H, Ar-H), 8.71 (d, 2H, Ar-H), 10.45 (s, 1H, NHNHCO). EI-MS: 354.7[M + H]⁺. Calcd. For C₁₇H₁₈N₆O₂S: C, 57.61; H, 5.12; N, 23.71; S, 9.05%. Found: C, 57.66; H, 5.14; N, 23.65; S, 9.04%.

General procedure for synthesis of compounds

4a–d

A mixture of compound **2** (0.2 mmol) and the corresponding nitrile (0.4 mmol) in dioxane (10 mL) was heated at 80 °C for 10 min; then, 15 mL of concentrated hydrochloric acid was added and reacted for 6 h. On completion of reaction (TLC), the mixture was cooled and poured onto cold water. The mixture was then basified with ammonium hydroxide. The solid obtained was filtered and purified by column chromatography on silica gel (Ethyl acetate/petroleum ether) to give **4a–d** as a solid.

4-Amino-2-methyl-5,6,7,8-tetrahydrobenzo[4,5]thieno[2,3-d]pyrimidine (4a)

Yellow solid, Yield: 59.1%; mp 224–225 °C; IR (cm⁻¹): 3470 (NH₂). ¹H-NMR (CDCl₃): δ 1.71–1.88 (m, 4H, TBTP-H), 2.41 (s, 3H, –CH₃), 2.73–2.84 (m, 2H, TBTP-H), 2.85–2.95 (m, 2H, TBTP-H), 5.01 (s, 2H, –NH₂). EI-MS: 220.3[M + H]⁺. Calcd. For C₁₁H₁₃N₃S: C, 60.24; H, 5.97; N, 19.16; S, 14.62%. Found: C, 60.27; H, 5.90; N, 19.21; S, 14.58%.

4-Amino-2-phenyl-5,6,7,8-tetrahydrobenzo[4,5]thieno[2,3-d]pyrimidine (4b)

Dark brown solid, Yield: 57.6%; mp 195–197 °C; IR (cm⁻¹): 3515 (NH₂). ¹H-NMR (DMSO-*d*₆): δ 1.71–1.87 (m, 4H, TBTP-H), 2.73–2.84 (m, 2H, TBTP-H), 2.85–2.94 (m, 2H, TBTP-H), 5.53 (s, 2H, –NH₂), 7.41–8.37 (m, 5H, Ph-H). EI-MS: 282.3[M + H]⁺. Calcd. For C₁₆H₁₅N₃S: C, 68.30; H, 5.37; N, 14.93; S, 11.40%. Found: C, 68.32H, 5.34; N, 14.90; S, 11.44%.

4-Amino-2-(4-hydroxyphenyl)-5,6,7,8-tetrahydrobenzo[4,5]thieno[2,3-d]pyrimidine (4c)

Brown solid, Yield: 36.6%; mp >250 °C; IR (cm⁻¹): 3529 (NH₂), 3100 (OH). ¹H-NMR (DMSO-*d*₆): δ 1.80–1.83 (m, 4H, TBTP-H), 2.71–2.80 (m, 2H, TBTP-H), 2.87–2.98 (m, 2H, TBTP-H), 6.71 (s, 2H, –NH₂), 6.81–6.87 (d, 2H, Ph-H, *J* = 7.4 Hz), 8.16–8.20 (d, 2H, Ph-H, *J* = 7.4 Hz), 9.76 (s, 1H, –OH). EI-MS: 297.6[M + H]⁺. Calcd. For C₁₆H₁₅N₃O₂S:

C, 64.62; H, 5.08; N, 14.13; S, 10.78%. Found: C, 64.65; H, 5.04; N, 14.17; S, 10.77%.

4-Amino-2-(4-methoxyphenyl)-5,6,7,8-tetrahydrobenzo[4,5]thieno[2,3-d]pyrimidine (4d)

Yellow solid, Yield: 39.7%; mp 200–202 °C; IR (cm⁻¹): 3491 (NH₂). ¹H-NMR (DMSO-*d*₆): δ 1.70–1.87 (m, 4H, TBTP-H), 2.73–2.86 (m, 2H, TBTP-H), 2.87–2.96 (m, 2H, TBTP-H), 3.91 (s, 3H, –OCH₃), 6.78 (s, 2H, –NH₂), 7.01–7.09 (d, 2H, Ph-H, *J* = 7.4 Hz), 7.92–7.98 (d, 2H, Ph-H, *J* = 7.3 Hz). EI-MS: 311.8[M + H]⁺. Calcd. For C₁₇H₁₇N₃O₂S: C, 65.57; H, 5.50; N, 13.49; S, 10.30%. Found: C, 65.63; H, 5.52; N, 13.40; S, 10.32%.

Synthesis of ethyl 2-amino-4,5,6,7-tetrahydrobenzo[b]thiophene-3-carboxylate (5)

Cyclohexanone (0.020 mol), sulfur (0.020 mol), ethyl cyanoacetate (0.020 mol), and ethanol (4 mL) were mixed and stirred together. To this mixture, diethylamine (0.025 mol) was added dropwise for up to half an hour and stirred continuously for another 3 h at room temperature. The reaction mixture was kept in a refrigerator overnight. The separated solid was filtered the next day, and washed with 4 mL of chilled 50% methanol to give **5** as light yellow crystals. Yield: 89.8%; mp 113–115 °C; IR (cm⁻¹): 3165 (NH), 2988 (CH), 1649 (C=O). ¹H-NMR (CDCl₃): δ 6.01 (s, 2H), 4.25 (q, 2H, *J* = 7.2 Hz), 2.71–2.69 (m, 2H), 2.48–2.46 (m, 2H), 1.75–1.73 (m, 4H), 1.33 (t, 3H, *J* = 7.2 Hz) (23,24).

Synthesis of 2-(chloromethyl)-4-hydroxy-5,6,7,8-tetrahydrobenzo[4,5]thieno[2,3-d]pyrimidine (6)

A mixture of compound **5** (1 g) and chloroacetonitrile (1 mL) in dioxane (15 mL) was heated at 80 °C for 10 min; then, 20 mL of concentrated hydrochloric acid was added and reacted for 6 h. On completion of reaction (TLC), the mixture was cooled and poured onto cold water. The mixture was then basified with ammonium hydroxide. The obtained solid was filtered, washed by methanol, dried, and crystallized from DMF to give **6** as a pale white crystalline solid (54.6%).

Synthesis of N'-[(4-hydroxy-5,6,7,8-tetrahydrobenzo[4,5]thieno[2,3-d]pyrimidin-2-yl)-methyl] isonicotin ohydrazide (7)

A mixture of compound **6** (0.2 mmol) and isoniazid (0.8 mmol) in dioxane (10 mL) was refluxed overnight. On completion of reaction (TLC), the solution was concentrated under reduced pressure and the residue was purified by column chromatography on silica gel (Ethyl acetate/petroleum ether) to give **7** as a yellow solid (66%). mp >250 °C; IR (cm⁻¹): 3300 (NH), 1655 (C=O). ¹H-NMR (DMSO-*d*₆): δ 1.74–1.82 (m, 4H, TBTP-H), 2.72–2.78 (m, 2H, TBTP-H), 2.88–2.90 (m, 2H, TBTP-H), 3.91 (s, 2H,

CH₂NH–), 7.84–7.85 (m, 2H, Ar-H), 8.16 (s, 1H, CHNHNH), 8.82 (m, 2H, Ar-H), 12.01 (s, 1H, NHNHCO), 12.61 (s, 1H, –OH). EI-MS: 356.2[M + H]⁺. Calcd. For C₁₇H₁₇N₅O₂S: C, 57.45; H, 4.82; N, 19.70; S, 9.02%. Found: C, 57.41; H, 4.89; N, 19.63; S, 8.97%.

Synthesis of 2-(4-hydroxyphenyl)-4-hydroxy-5,6,7,8-tetrahydrobenzo[4,5]thieno[2,3-d]pyrimidine (8)

A mixture of compound **5** (1 g) and 4-hydroxybenzonitrile (2 g) in dioxane (15 mL) was heated at 80 °C for 10 min; then, 20 mL of concentrated hydrochloric acid was added and reacted for 6 h. On completion of reaction (TLC), the mixture was cooled and poured onto cold water. The mixture was then basified with ammonium hydroxide. The obtained solid was filtered and purified by column chromatography on silica gel (Ethyl acetate/petroleum ether) to give **8** as a white solid (35.1%). Mp >250 °C; IR (cm⁻¹): 3100 (NH), 3095 (OH). ¹H-NMR (DMSO-*d*₆): δ 1.70–1.78 (m, 4H, TBTP-H), 2.71–2.80 (m, 2H, TBTP-H), 2.85–2.90 (m, 2H, TBTP-H), 6.84–6.89 (d, 2H, Ph-H, *J* = 7.2 Hz), 7.96–8.04 (d, 2H, Ph-H, *J* = 7.2 Hz), 10.21 (s, 1H, Ph-OH), 12.30 (s, 1H, TBTP-NH₂). EI-MS: 299.4[M + H]⁺. Calcd. For C₁₆H₁₄N₂O₂S: C, 64.41; H, 4.73; N, 9.39; S, 10.75%. Found: C, 64.35; H, 4.67; N, 9.49; S, 10.83%.

In vitro FGFR-1 kinase assays

The ability of all target compounds to inhibit the activation of FGFR1 kinase domain was detected by Caliper Mobility Shift Assay on EZ Reader (Caliper Life Sciences, Hopkinton, MA, USA). According to the instructions provided, the concentration of compounds was 10 μM, and the reference inhibitor staurosporine (Sigma, St. Louis, MO, USA) was used as the control.

MTT Assay for antitumor activity at the cellular level

The MTT assay was performed to evaluate the cytotoxic and antiproliferative activities of all compounds. Three cell lines (A549, H460 and U251) were seeded (2000–20 000 cells per well) in 96-well plates, respectively. After incubation for 24 h in serum-containing media, the cells were treated with inhibitors (50, 10, 2, and 0.4 μM), diluted with a culture medium for 24 h at 37 °C under a 5% CO₂ atmosphere. Thereafter, 20 μL of the MTT reagent (5 mg/mL; Sigma) was added to each well, and the plates were incubated for 4 h at 37 °C. Finally, the absorbance at 490 nm was read using an ELX800 microplate reader. Compound **16** was used as the positive control, and DMSO was used as negative control. All experiments were performed parallel in triplicate.

Docking

To gain further insight into the interaction mode between these derivatives and FGFRs, molecular docking analysis

was performed by AutoDock version 4.2 (25). A crystal structure (Protein Data Bank code: 3JS2) was selected for the construction of the docking template (26). To better prepare the target protein as a template, the ligand and crystallographic water were removed. Subsequently, compounds **3g** and **4c** were chosen to dock with the validated template.

Statistical analysis

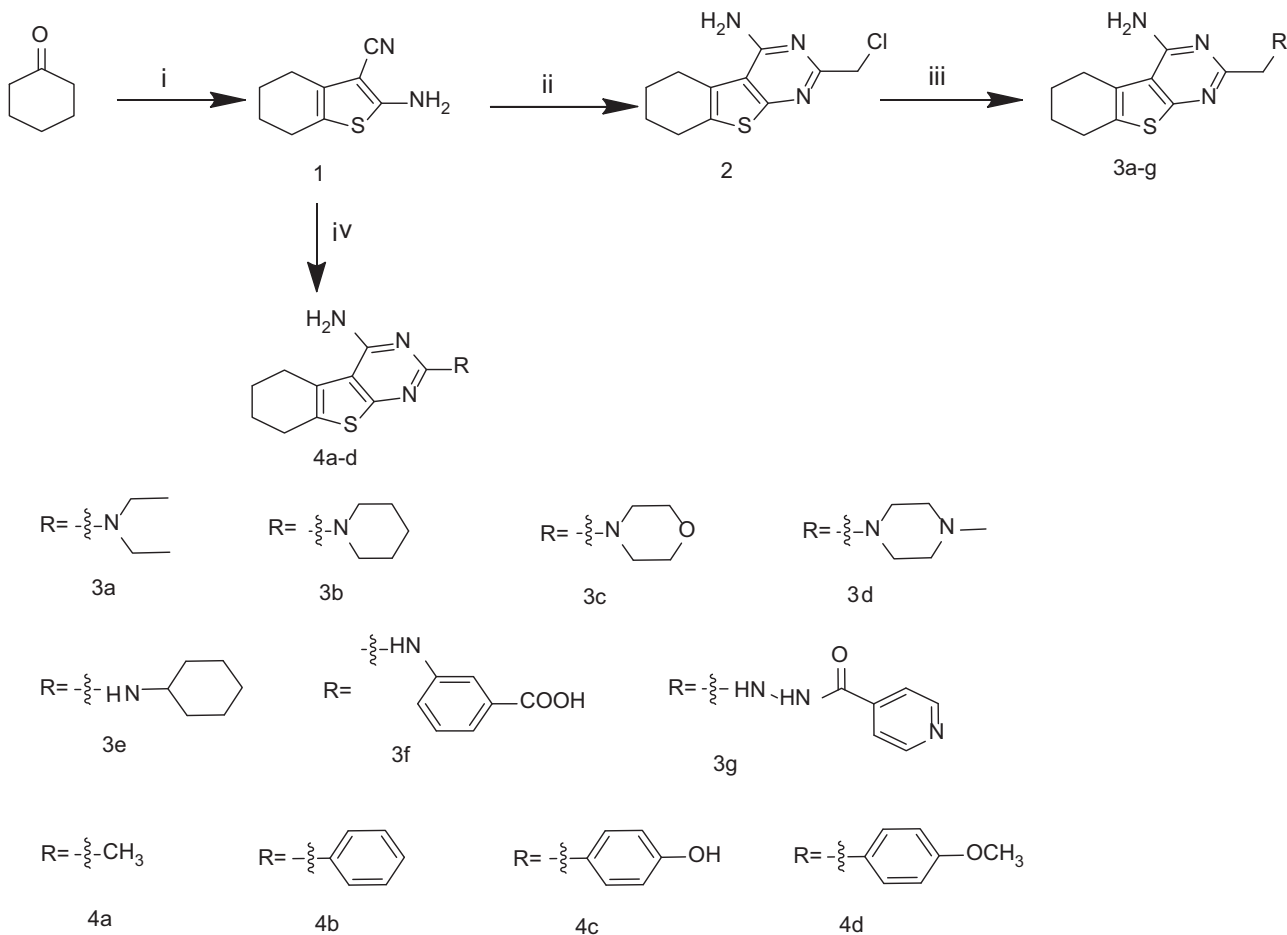
Data were presented as mean \pm SD of three parallel measurements. Statistical significance was analyzed using a two-tailed Student's *t*-test for comparison of two groups. In all cases, post hoc comparisons of the means of individual groups were performed using one-way analysis of variance (ANOVA). $p < 0.05$ was considered as significant. All statistical analyses were performed by GraphPad Prism version 5.0 (GraphPad Inc., San Diego, CA, USA) or Statistical Product and Service Solutions version 16.0 (SPSS Inc., Chicago, IL, USA). For data analysis: IC₅₀ values were obtained using GraphPad Prism version 5.0 (GraphPad Inc.).

Results and Discussion

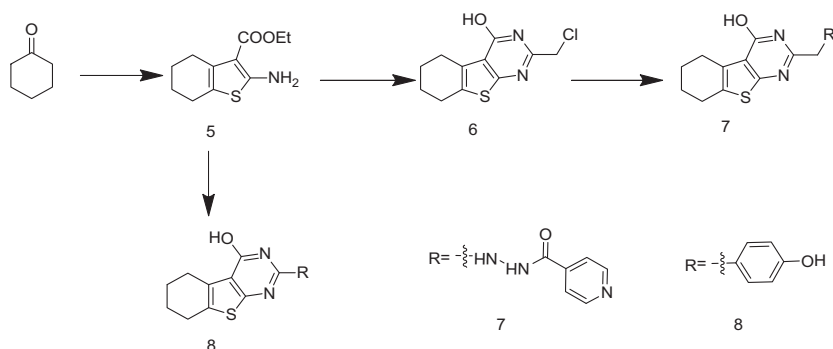
Chemistry

Based on the core scaffold of 5,6,7,8-tetrahydrobenzo[4,5]thieno[2,3-d]pyrimidine, 13 compounds **3a–g**, **4a–d**, **7**, and **8** were designed and synthesized. Among these, 7 compounds (**3a**, **3b**, **3e**, **3f**, **3g**, **4c**, and **7**) are first reported here. These target compounds were further characterized by physicochemical and spectral studies (IR, ¹H NMR, ESI-MS). IR spectra showed characteristic bands of amide (3200–3500 cm^{−1}). The ¹H spectrum was carried out at 600 MHz and showed a characteristic peak pattern. Synthetic pathways of the designed compounds were shown in Schemes 1 and 2, respectively.

Structural optimization was performed by focusing on the C-2 position of the tetrahydrobenzothienopyrimidine scaffold. The influence of key factors, such as reaction temperature, and the yield of the target compounds were investigated. The key intermediate of 2-amino-4,5,6,7-tetrahydrobenzo[b]thiophene-3-carbonitrile (**1**) was pre-



Scheme 1: Route for the synthesis of 4-amino-tetrahydrobenzothieno[2,3-d]pyrimidine derivatives **3a–g**, **4a–d**. *Reagents and conditions:* (i) sulfur, malononitrile, morpholine, ethanol, 60 °C, 12 h; (ii) chloroacetonitrile, conc HCl, dioxane, 80 °C, 6 h; (iii) amine, dioxane, reflux, 20 h; (iv) RCN, HCl, dioxane, 80 °C, 12 h.



Scheme 2: Route for the synthesis of tetrahydrobenzothieno[2,3-d]pyrimidine-4-one derivatives **7** and **8**. *Reagents and conditions:* (i) sulfur, ethyl cyanoacetate, morpholine, ethanol, 60 °C, 12 h; (ii) chloroacetonitrile, conc HCl, dioxane, 80 °C, 6 h; (iii) amine, dioxane, reflux, 20 h; (iv) RCN, HCl, dioxane, 80 °C, 12 h.

pared by means of a Gewald's reaction (19,26). 4-amino-2-chloromethyl-5,6,7,8-tetrahydrobenzo[4,5]thieno[2,3-d]pyrimidine (**2**) was prepared with an excellent yield by treating **1** with chloroacetonitrile in dioxane at 80 °C. The reaction of 4-amino-2-chloromethyl-5,6,7,8-tetrahydrobenzo[4,5]thieno[2,3-d]pyrimidine (**2**) with various nitriles afforded 4-amino-5,6,7,8-tetrahydrobenzo[4,5]thieno[2,3-d]pyrimidine (**3a–g**) at 35–61% yields. Similarly, compounds (**4a–d**) were prepared by 2-amino-4,5,6,7-tetrahydrobenzo[b]thiophene-3-carbonitrile (**1**) with various nitriles. Spectral data of all synthesized compounds were in full agreement with the proposed structures.

Inhibition of FGFR1 kinase activity *in vitro*

All compounds were screened by Caliper Mobility Shift Assay on EZ Reader (Caliper Life Sciences) on kinase FGFR1 *in vitro* while staurosporine was used as the reference compound. As shown in Figure 2, the general trend showed that the majority of the analogs tested appeared to show concentration-dependent inhibition to FGFR1. Compounds **3g**, **4c**, and **7** showed the highest potency whether at 10, 1, or 0.1 μM . One suggestion put forward was that the results could be due to the space structure of the ATP site of FGFR1, which was large enough to contain larger molecules and formed more bonds with these molecules. Among the tested compounds, **3g** exhibited the best performance at a concentration of 10 μM .

Antitumor activities *in vitro* based on MTT assay

All synthesized compounds were further screened for their antitumor activities *in vitro*. Three cancer cell lines known to express high levels of FGFR1 were tested in MTT assay including H460, A549, and U251 (27,28). The data were summarized in Table 1. The results indicated that compounds showed different antitumor activities, which corresponded to the inhibition of FGFR1. Compound **3g** displayed good activities against all three cells (H460, A549, and U251) with IC_{50} values of 7.7, 18.9, and 13.3 μM , respectively.

Docking

The docking results revealed that compound **4c** formed two hydrogen bonds with the hydroxyl oxygen of Lys-514 and Asp-64, the distance between is 3.1 and 2.0 Å, respectively (Figure 3A); while compound **3g** formed six hydrogen bond, its carbonyl oxygen being hydrogen-bonded by the side chains of Asn-568 and Glu-571, hydrogen to nitrogen being hydrogen-bonded by the side chains of Ala-564, Leu484, and Gly-487 (Figure 3B). It was different to the reference, and ligands were bind in the hinge region and featured two hydrogen bonds with Ala564 via the amido fragments ($\text{O}=\text{C}-\text{NH}$) in the pseudothiohydantoin and pyrimidinone rings (26). Although compound **3g** formed more hydrogen bonds than compound **4c**, the distance of the hydrogen bonds were

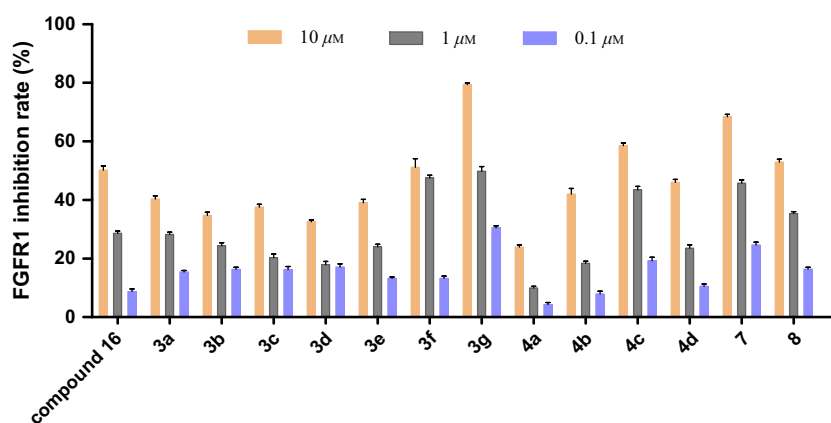
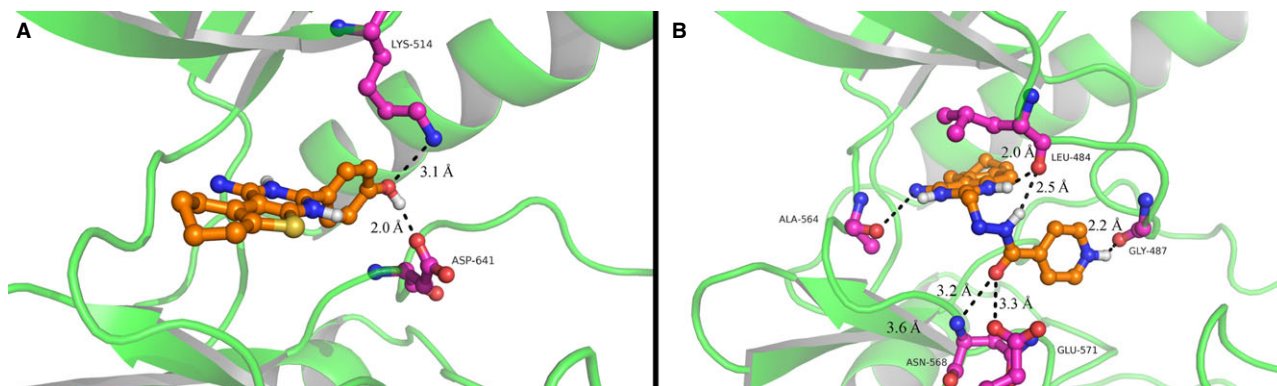


Figure 2: Inhibition of FGFR1 kinase activity by the tested compounds *in vitro*. The activity of all synthesized compounds toward in inhibiting FGFR1 kinase activity was determined by Caliper Mobility Shift Assay on EZ Reader.

Table 1: The IC₅₀ values for the tested compounds on cell proliferation based on MTT assay

Compounds	IC ₅₀ values/ μ M		
	H460	A549	U251
Compound 16	32.6 \pm 1.9	47.1 \pm 1.2	86.3 \pm 2.1
3a	260.6 \pm 10.5***	328.6 \pm 0.7***	361.4 \pm 8.2***
3b	236.4 \pm 0.2***	131.2 \pm 1.7***	>1000***
3c	>1000***	347.7 \pm 12.0***	287.0 \pm 12.5***
3d	161.3 \pm 13.7***	288.2 \pm 8.7***	149.3 \pm 1.5***
3e	87.2 \pm 2.5***	75.6 \pm 2.6***	102.4 \pm 5.3***
3f	25.1 \pm 0.8###	38.3 \pm 2.5###	27.6 \pm 2.3###
3g	7.7 \pm 2.1###	18.9 \pm 2.3###	13.3 \pm 2.4###
4a	>1000***	346.7 \pm 11.0***	>1000***
4b	98.3 \pm 8.4***	256.8 \pm 18.9***	87.1 \pm 8.2
4c	41.3 \pm 3.4***	89.6 \pm 6.2***	37.2 \pm 2.3***
4d	84.3 \pm 1.5***	74.6 \pm 1.1***	56.4 \pm 1.7***
7	19.1 \pm 1.3###	23.1 \pm 1.8###	21.0 \pm 1.6###
8	69.5 \pm 1.4***	86.9 \pm 2.1***	85.6 \pm 1.5

Each value represents the mean \pm SEM from three experiments significantly different from compound 16 at ***p < 0.001 (Student's *t*-test). ### stands for compounds which show significantly higher activity than compound **16**. Bold value shows the most active compound.


Figure 3: Computed binding geometry of the new inhibitors Compound **4c** and **3g**, with the FGFR1 ATP-binding pocket.(A: Compound **4c** formed 2 hydrogen bonds. B: Compound **3g** formed 6 hydrogen bonds).

farther away. Also the free energies of binding were -7.22 kcal/mol (**3g**) and -8.97 kcal/mol (**4c**). It was obvious that docking results were consistent with the activity.

Structure–activity relationship

Considering the whole results, we here analyze the structure–activity relationship (SAR). Firstly, compare **3g** with **7**, we found $-\text{NH}_2$ is more favorable than $-\text{C}=\text{O}$ in the C-4 position, this was opposite to the original intention. Secondly, the activities were slightly affected by the type of the substituents on the C-2 position (see **3a**, **3b**, **3c**, **3d**, and **4a**). Thirdly, compared **4a** with **4b**, one can see aromatic substituted showed more positive activities than methyl. Furthermore, activities appeared significantly increase when C-2 position is substituted by 4-hydroxy-

phenyl (see **4c**). For all, **3g** showed a significantly affect on inhibiting the FGFR than any other compounds.

Conclusion

In summary, a new class of tetrahydrobenzothienopyrimidine derivatives were designed, synthesized, and evaluated for their antitumor activity in various cancer cells with high FGFR1 kinase activity. Although most compounds showed a different inhibition of FGFR1, the compound **3g** showed better activity toward FGFR1 in this research, suggesting that compounds with side chains substituted with larger groups exhibited better activity. This could be due to the space structure of the FGFR1 ATP pocket, which was large enough to accommodate larger molecules and could form more bonds with these molecules. The results

of this article has broaden the application of tetrahydrobenzothieno[2,3-*d*]pyrimidine core.

Acknowledgments

This work was supported by the National Natural Science Foundation of China (81373262) for financial support. The IR, ¹H-NMR, and ESI-MS were recorded by the Analysis and Test Center of Wenzhou Medical University.

Conflict of Interest

The authors confirm that this article content has no conflict of interests.

References

- Turner N., Grose R. (2010) Fibroblast growth factor signalling: from development to cancer. *Nat Rev Cancer*;10:116–129.
- Strawn L.M., Shawver L.K. (1998) Tyrosine kinases in disease: overview of kinase inhibitors as therapeutic agents and current drugs in clinical trials. *Expert Opin Investig Drugs*;7:553–573.
- Liang G., Chen G., Wei X., Zhao Y., Li X. (2013) Small molecule inhibition of fibroblast growth factor receptors in cancer. *Cytokine Growth Factor Rev*;24:467–475.
- Gessi M., Moneim Y.A., Hammes J., Goschzik T., Scholz M., Denkhau D., Pietsch T. (2014) FGFR1 mutations in Rosette-forming glioneuronal tumors of the fourth ventricle. *J Neuropathol Exp Neurol*;73:580–584.
- Guagnano V., Furet P., Spanka C., Bordas V., Le Douget M., Stamm C., Graus Porta D. (2011) Discovery of 3-(2, 6-dichloro-3, 5-dimethoxy-phenyl)-1-{6-[4-(4-ethyl-piperazin-1-yl) -phenylamino]-pyrimidin-4-yl}-1-methyl-urea (NVP-BGJ398), a potent and selective inhibitor of the fibroblast growth factor receptor family of receptor tyrosine kinase. *J Med Chem*;54:7066–7083.
- Hafez H.N., Hussein H.A., El-Gazzar A.R.B. (2010) Synthesis of substituted thieno [2, 3-*d*] pyrimidine-2,4-dithiones and their S-glycoside analogues as potential antiviral and antibacterial agents. *Eur J Med Chem*;45:4026–4034.
- Verheijen J.C., Yu K., Toral-Barza L., Hollander I., Zask A. (2010) Discovery of 2-arylthieno [3,2-*d*] pyrimidines containing 8-oxa-3-azabi-cyclo[3.2.1]octane in the 4-position as potent inhibitors of mTOR with selectivity over PI3K. *Bioorg Med Chem Lett*;20:375–379.
- Yang F., Zhang Y., Ressler S.J., Ittmann M.M., Ayala G.E., Dang T.D., Rowley D.R. (2013) FGFR1 is essential for prostate cancer progression and metastasis. *Cancer Res*;73:3716–3724.
- Weiss J., Sos M.L., Seidel D., Peifer M., Zander T., Heuckmann J.M., Damiani S. (2010). Frequent and focal FGFR1 amplification associates with therapeutically tractable FGFR1 dependency in squamous cell lung cancer. *Sci Transl Med*, 2, 62ra93.
- Ye F., Chen L., Hu L., Xiao T., Yu S., Chen D., Wang S. (2015) Design, synthesis and preliminary biological evaluation of C-8 substituted guanine derivatives as small molecular inhibitors of FGFRs. *Bioorg Med Chem Lett*;25:1556–1560.
- Ye F., Wang Y., Nian S., Wang Y., Chen D., Yu S., Wang S. (2015) Synthesis and evaluation of biological and antitumor activities of 5,7-dimethyl-oxazolo [5,4-*d*] pyrimidine-4,6(5H, 7H)-dione derivatives as novel inhibitors of FGFR1. *J Enzyme Inhib Med Chem*. doi:10.3109/14756366.2014.1002401
- Fearon A.E., Gould C.R., Grose R.P. (2013) FGFR signalling in women's cancers. *Int J Biochem Cell Biol*;45:2832–2842.
- Zhou W., Hur W., McDermott U., Dutt A., Xian W., Ficarro S.B., Gray N.S. (2010) A structure-guided approach to creating covalent FGFR inhibitors. *Chem Biol*;17:285–295.
- Wang Y., Cai Y., Ji J., Liu Z., Zhao C., Zhao Y., Liang G. (2014) Discovery and identification of new non-ATP competitive FGFR1 inhibitors with therapeutic potential on non-small-cell lung cancer. *Cancer Lett*;344:82–89.
- Kumar B.V.S., Narasu L., Gundla R., Dayam R., Jarp S. (2013) Fibroblast growth factor receptor inhibitors. *Curr Pharm Des*;19:687–701.
- Liang G., Liu Z., Wu J., Cai Y., Li X. (2012) Anticancer molecules targeting fibroblast growth factor receptors. *Trends Pharmacol Sci*;33:531–541.
- Al-Duaij O.K., Hafez H.N., El-Gazzar A.R.B.A. (2013) Synthesis of Novel Series of Benzothieno [2,3-*d*] Pyrimidine Derivatives, Promising Anticancer Agents. *J Chem Chem Eng*;7:725–742.
- Wu C.H., Coumar M.S., Chu C.Y., Lin W.H., Chen Y.R., Chen C.T., Hsieh H.P. (2010) Design and synthesis of tetrahydropyridothieno [2, 3-*d*] pyrimidine scaffold based epidermal growth factor receptor (EGFR) kinase inhibitors: the role of side chain chirality and Michael acceptor group for maximal potency. *J Med Chem*;53:7316–7326.
- Abbas S.E., Gawad N.M.A., George R.F., Akar Y.A. (2013) Synthesis, antitumor and antibacterial activities of some novel tetrahydrobenzo [4,5] thieno [2,3-*d*] pyrimidine derivatives. *Eur J Med Chem*;65:195–204.
- Dave C.G., Shah R.D. (1998) Synthesis of 7H-tetrazolo [1,5-*c*]pyrrolo[3,2-*e*]pyrimidines and their reductive ring cleavage to 4-aminopyrrolo[2,3-*d*]pyrimidines. *J Heterocycl Chem*;35:1295–1300.
- Sabnis R.W., Rangnekar D.W., Sonawane N.D. (1999) 2-Aminothiophenes by the Gewald reaction. *J Heterocycl Chem*;36:333–345.
- Mulla J.A.S., Khazi M.I.A., Panchamukhi S.I., Gong Y.D., Khazi I.A.M. (2014) Synthesis and pharmacological evaluation of novel thienopyrimidine and triazolothienopyrimidine derivatives. *Med Chem Res*;23: 3235–3243.

23. Mojtahedi M.M., Abaee M.S., Mahmoodi P., Adib M. (2010) Convenient synthesis of 2-aminothiophene derivatives by acceleration of Gewald reaction under ultrasonic aqueous conditions. *Synth Commun*;40: 2067–2074.
24. Haswani N.G., Bari S.B. (2011) Synthesis and antimicrobial activity of novel 2-(pyridin-2-yl) thieno [2,3-d] pyrimidin-4(3H)-ones. *Turk J Chem*;35:915–924.
25. Morris G.M., Huey R., Lindstrom W., Sanner M.F., Belew R.K., Goodsell D.S., Olson A.J. (2009) AutoDock4 and AutoDockTools4: automated docking with selective receptor flexibility. *J Comput Chem*;30: 2785–2791.
26. Ravindranathan K.P., Mandiyan V., Ekkati A.R., Bae J.H., Schlessinger J., Jorgensen W.L. (2010) Discovery of novel fibroblast growth factor receptor 1 kinase inhibitors by structure-based virtual screening. *J Med Chem*;53:1662–1672.
27. Yang J., Zhao H., Xin Y., Fan L. (2014) MicroRNA-198 Inhibits Proliferation and Induces Apoptosis of Lung Cancer Cells Via Targeting FGFR1. *J Cell Biochem*;115:987–995.
28. Wu X., Huang H., Wang C., Lin S., Huang Y., Wang Y., Li X. (2013) Identification of a novel peptide that blocks basic fibroblast growth factor-mediated cell proliferation. *Oncotarget*;4:1819.